

GRB 121027A: LONG-LASTING, ENERGETIC X-RAY FLARES AND CLUES TO RADIATION MECHANISM AND PROGENITOR STAR

FANG-KUN PENG¹, YOU-DONG HU¹, SHAO-QIANG XI¹, XIANG-GAO WANG¹, RUI-JING LU¹, EN-WEI LIANG^{1,2} AND BING ZHANG^{3,1}

ABSTRACT

GRB 121027A is unusual with its extremely long-lasting, energetic X-ray flares. The total energy release in X-ray flares is about one order of magnitude higher than prompt γ -rays, making it special from most long GRBs. We show that while the prompt gamma-ray emission satisfies the empirical $E_{\text{iso}} - E_p$ relation of typical long GRBs, the X-ray flares, whose spectra can be fit with a cutoff-power-law model with well-constrained E_p , significantly deviate from such a relation. Nonetheless, a time-resolved spectral analysis of X-ray flares suggest that the X-ray emission is consistent with the $L_{\text{iso}} - E_p$ relation of long GRBs. We constrain the minimum Lorentz factor of the X-ray flares to be ~ 14 , which is consistent with the $\Gamma - L_{\text{iso}}$ relation. Our results imply that prompt γ -ray emission and late X-ray flares share the similar radiation mechanism, but originate from the outflows with different Lorentz factors. We search for similar GRBs from the *Swift* GRB archives, and find that the $z = 6.29$ GRB 050904 is a carbon copy of GRB 121027A. The long-lasting, energetic X-ray flares in these GRBs demand significant accretion at late times, which point towards a large-radius progenitor star.

Subject headings: radiation mechanisms: non-thermal — gamma-ray burst: individual (121027A)

1. INTRODUCTION

Observations with *Swift* mission has greatly improved our understanding on the nature of the gamma-ray burst (GRB) phenomenon. The rapid slewing capacity of the X-ray telescope (XRT) onboard *Swift* makes it possible to catch X-ray emission from very early to late epochs of GRBs. A large sample of GRB X-ray lightcurves have been collected in the time window from tens of seconds to days or even months post the Burst Alert Telescope (BAT) triggers. A canonical X-ray lightcurve with five components was revealed from the sample (Zhang et al. 2006; Nousek et al. 2006)⁴.

X-ray flares are observed for about half of the Swift GRBs (Burrows et al. 2005; Falcone et al. 2007; Chincarini et al. 2007). Most flares happened at $t < 1000$ seconds and a small fraction of flares occurred at $\sim 10^5$ seconds post the GRB trigger time (T_0). No significant flare after the prompt gamma-ray phase was detected for about 1/3 of these GRBs, but bright X-ray flares were detected for the other 2/3 of GRBs (Qin et al. 2013). Joint spectral analyses for the prompt gamma-ray emission and early X-ray flares indicate that X-ray flares are the low-energy extension of the prompt gamma-ray emission (Peng et al. 2013). Significant flares that dominate late X-ray emission (without the detection of the afterglow emission up to $\sim 10^5$ seconds) were observed in some GRBs, such as GRBs 050502B, 050724, 050904, and 060223. The most prominent one is GRB 050904 (Cusumano et al. 2007), which was suggested as a super-

long GRB (Zou et al. 2006). It is generally believed that these X-ray flares are due to extended central engine activity at late times (Burrows et al. 2005; Zhang et al. 2006; Fan & Wei 2005; King et al. 2005; Dai et al. 2006; Perna et al. 2006; Proga & Zhang 2006; Liang et al. 2006; Lazzati & Perna 2007). Late flares may be critical for revealing the global evolution of the GRB central engine, hence the properties of the progenitor stars. It is unclear whether the X-ray flares share the relations between spectral peak energy (E_p) and burst energetics that have been found for long GRBs with the prompt γ -ray data, such as the $E_{\gamma, \text{iso}} - E_p$ relation (the Amati-relation; Amati et al. 2002) and the $L_{\gamma, \text{iso}} - E_p$ relation (Yonetoku et al. 2004; Liang et al. 2004), where $E_{\gamma, \text{iso}}$ (or $L_{\gamma, \text{iso}}$) is the bolometric isotropic gamma-ray energy release (or luminosity) in a wide band ($1 - 10^4$ keV).

Swift/BAT triggered an unusual GRB on Oct. 27, 2012, which has extremely bright and long flares that last up to $\sim 10^5$ s post the GRB trigger (Evans et al. 2012). Here we present an analysis of GRB 121027A in order to study whether the late flares share the same relations with the prompt gamma-rays. The concordance cosmology with parameters $H_0 = 71 \text{ km s}^{-1} \text{ Mpc}^{-1}$, $\Omega_M = 0.30$, and $\Omega_\Lambda = 0.70$ is adopted to calculate burst energetics.

2. DATA ANALYSIS RESULTS

GRB 121027A has a redshift 1.773 (Levan et al. 2012). We downloaded the BAT and XRT data from the *Swift* archive⁵, and extracted the lightcurves and spectra in the BAT and XRT bands. The 0.3-10 keV band lightcurve is shown in Fig. 1, with XRT data directly plotted and the BAT data extracted to this energy band based on its spectral information in the BAT band. The duration T_{90} in the BAT band is 62.6 ± 4.8 seconds. A steep decay segment from $T_0 + 70$ to $T_0 + 180$ seconds is observed

¹ Department of Physics and GXU-NAOC Center for Astrophysics and Space Sciences, Guangxi University, Nanning, Guangxi 530004, China; lew@gxu.edu.cn

² National Astronomical Observatories, Chinese Academy of Sciences, Beijing 100012, China

³ Department of Physics and Astronomy, University of Nevada Las Vegas, Las Vegas, NV 89154, USA

⁴ The X-ray lightcurves of a small fraction of GRBs are a featureless single power-law (Liang et al. 2009; Evans et al. 2009).

⁵ <http://heasarc.nasa.gov/docs/swift/archive/>

in the XRT band. Bright X-ray flares are observed during $T_0 + 180$ and $T_0 + 4 \times 10^4$ seconds. The first flare peaks at around $T_0 + 270$ seconds. After a dip, the flux rises rapidly with a slope $\alpha > 10$. The peak of the 2nd flare was not detected because of the orbit constraint. The MAXI/GSC nova alert system triggered on a bright un-catalogued X-ray transient source with 4-10 keV flux about 150 mCrab at $T_0 + 2400$ seconds, and the transient was identified as the X-ray emission from GRB 121027A (Serino et al. 2012). We correct the flux to the 0.3-10 keV energy band and also show it in Fig. 1. The third flare peaks around $T_0 + 7 \times 10^3$ seconds. The flux from $T_0 + 5300$ to $T_0 + 5600$ seconds almost keeps constant, which maybe due to superposition of the tail of the second flare and the rising segment of the third flare. We make an empirical fit to the three flares with three broken power-law components, as shown in Fig. 1. One can observe that the peak luminosities of the three flares do not show a clear evolution pattern. After the flaring phase, a plateau between $T_0 + 4 \times 10^4$ and $T_0 + 1.5 \times 10^5$ seconds is observed. It transits to a decay segment with a slope $\alpha = -1.55$ up to 3×10^6 seconds.

The BAT spectrum is well fit with a single power-law, which yields a photon spectral index $\Gamma_{\text{BAT}} = 1.97 \pm 0.07$ and a reduced $\chi^2 = 40/56$ dof. XRT detected the corresponding X-rays of prompt emission from $T_0 + 57$ to $T_0 + 66$ seconds in the slewing mode. We make a joint spectral analysis of the spectrum accumulated with BAT and XRT in the prompt emission phase, and find that the spectrum is well fit with a cutoff power-law, with low energy photon index $\Gamma_\gamma = 1.49^{+0.11}_{-0.12}$ and cutoff energy $E_c = 93^{+56}_{-27}$ keV (corresponding to an $E_p = 47^{+30}_{-17}$ keV), as shown in Fig. 2(a).

We perform a time-resolved spectral analysis of the XRT data. In our spectral fitting, the absorption of our Galaxy is fixed as $N_H = 0.015 \times 10^{22} \text{ cm}^{-2}$. In order to avoid artificial N_H variations for the GRB host galaxy caused by the intrinsic spectral evolution that commonly observed in the brightest X-ray flares (Butler & Kocevski 2007), we fix the host galaxy absorption to $N_H^{\text{host}} = 1.26 \times 10^{22} \text{ cm}^{-2}$, which is derived from fitting the late time spectrum between $T_0 + 16347$ and $T_0 + 76223$ s. We find that although a single power-law model can present acceptable fits for the time-resolved spectra during the flares, a cut-off power-law model significantly improves the spectral fits for some time intervals of the flares. We compare our spectral fit results with the two models in Table 1. One example of our spectral fit with an absorbed cutoff power-law model is shown in Fig. 2(b). We adopt the cut-off power-law model fits, if their C-statistic is smaller than that of the single power-law fits with ~ 20 , as marked with a “ \checkmark ” in Table 1.

The E_p or power-law photon index (Γ) evolution is shown in Fig. 1. One can see that E_p rapidly decays from 47 ± 13 keV down to ~ 1 keV during the steep decay phase of the last pulse, being well consistent with the tail emission of the prompt emission as observed in other GRBs (e.g. Zhang et al. 2007). The time-resolved spectra of X-ray afterglows after $t > 4 \times 10^5$ are well fit with an absorbed power-law with photon spectral index $\sim (2.2-2.5)$, being well consistent with most other GRBs (e.g. Liang et al. 2007).

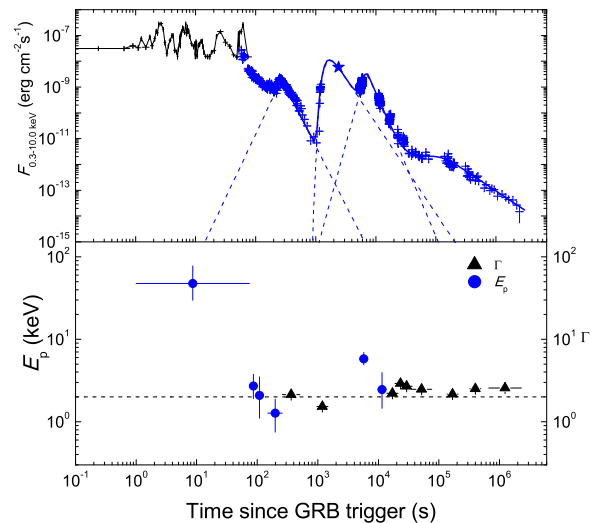


FIG. 1.— Lightcurve in the 0.3-10 keV band and E_p or power-law photon index (Γ) evolution of GRB 121027A derived from observations with BAT and XRT. The empirical fit for lightcurve of the late flares are also shown. Dashed lines are fits to individual flares and the solid line represents the sum of all flares. The horizontal dashed line marks $\Gamma = 2$.

3. EMPIRICAL RELATIONS

We correct the observed $E_{\gamma, \text{iso}}$ to the $1 - 10^4$ keV band with the spectral parameters reported above. We obtain $E_{\gamma, \text{iso}} = (2.86 \pm 0.23) \times 10^{52}$ erg, where the error is calculated by a bootstrap method assuming the error of photon index Γ has a normal distribution and the errors of both E_p and S_γ have log-normal distributions.

In Fig. 3(a), we plot GRB 121027A in the $E_{\gamma, \text{iso}} - E_p$ diagram and find that it well follows the empirical Amati-relation. We then test if the flares at $t > T_0 + 200$ seconds are also consistent with this relation. We calculate the X-ray fluence in the 0.3-10 keV by integrating the X-ray flux over three flares with the spectral parameters derived above. We obtain an X-ray fluence $S_X = 2.51 \times 10^{-5}$ erg cm^{-2} , which corresponds to an isotropic X-ray energy $E_{X, \text{iso}} = 1.89 \times 10^{53}$ erg. Note that we do not correct the X-ray energy to the $1 - 10^4$ keV band, since the 0.3-10 keV band spectrum can be well fit with a cutoff power-law, so that fluence above E_p is negligible. We can see that the total energy of the flares is about one order of magnitude larger than the gamma-ray energy, but E_p values of the X-ray flares are much lower than those of gamma-rays. As shown in Fig. 3(a), the flares significantly deviate from the Amati-relation. Next, with a time-resolved spectral analysis, we plot $L_{X, \text{iso}}$ as a function of E_p in Fig. 3(b). It is interesting to see that the time-resolved $L_{X, \text{iso}}$ and E_p are consistent with the $L_{\text{iso}} - E_p$ correlation for long GRBs (Yonetoku et al. 2004; Liang et al. 2004). These results suggest that the radiation mechanism of prompt gamma-rays and late X-rays is likely the same, even though the luminosity and energetics are noticeably different.

After the flare phase, a long-lasting X-ray plateau was observed during $T_0 + 4 \times 10^4 - T_0 + 1.3 \times 10^5$. This is likely the emission from the external forward shock, which is constantly refreshed by the new ejected materials that

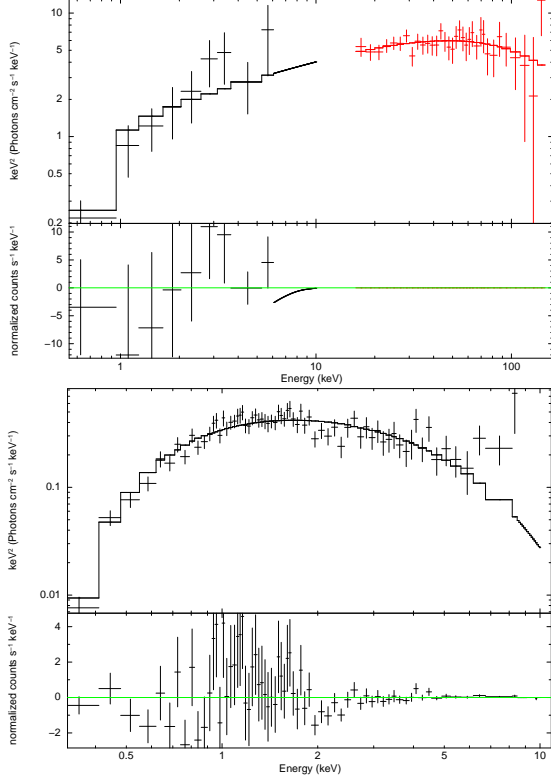


FIG. 2.— *top panel*: Joint spectral fit for the data observed with BAT and XRT for the prompt gamma-rays. *bottom panel*: Example of our absorbed cut-off power-law model fit to the spectrum of the flare data in time interval $T_0 + 150 \sim 260$ s.

power the X-ray flares. The end of the plateau marks the end of this energy injection, which is defined by the lower limit of the Lorentz factor of the late ejecta. This can be estimated by (Zhang et al. 2006)

$$\Gamma_m = 23E_{X,iso,52}^{1/8} n^{-1/8} t_{b,4}^{-3/8} [(1+z)/2]^{3/8}, \quad (1)$$

which gives $\Gamma_m \sim 14$ for GRB 121027A. This minimum Lorentz factor, even though violates the $\Gamma - E_{iso}$ correlation (Liang et al. 2010), is consistent with the $\Gamma - L_{iso}$ correlation (Lü et al. 2012) within 2σ confidence level. Lei et al. (2013) have shown that this correlation is more fundamental, and is directly connected to the GRB central engine physics.

4. PHYSICAL IMPLICATIONS ON RADIATION MECHANISM AND PROGENITOR

The fact that X-ray flares follow the same $L_{iso} - E_p$ and $\Gamma - L_{iso}$ relations as prompt emission suggest that the radiation mechanism of X-ray flares and prompt gamma-ray emission is similar. The difference is that the more powerful prompt emission has a higher Lorentz factor than X-ray flares. The radiation mechanism of prompt emission is not clear. In the literature, competing models include synchrotron radiation (Mészáros et al. 1994; Lloyd & Petrosian 2000; Zhang & Yan 2011) and quasi-thermal emission from the fireball photosphere (e.g. Thompson 1994; Rees & Mészáros 2005; Beloborodov 2010; Lazzati & Begelman 2010). At a low accretion rate that is relevant to X-ray flares, the neutrino-anti-neutrino annihilation mechanism would not be adequate to power X-ray flares, and magnetic dissipation is favored (e.g. Fan et al. 2005). As a result, synchrotron

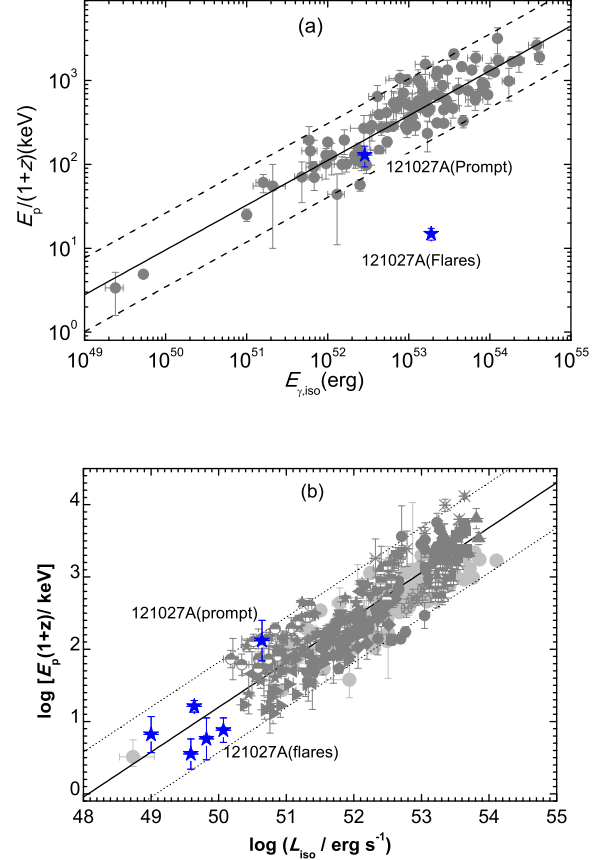


FIG. 3.— GRB 121027A prompt gamma-ray and X-ray flares against empirical correlations of other long GRBs: (a) the Amati relation; (b) the time-resolved $L_{\gamma,iso} - E_p$ relation. The data of the typical GRBs (grey dots) are from Amati et al. (2009), Lu et al. (2012) and references therein. Lines are the best fits and the dashed lines mark the 2σ region of the correlations.

emission from a magnetized jet may be the common mechanism to power both prompt emission and X-ray flares.

Long GRBs are widely believed to be associated with the deaths of massive stars (Colgate 1974; Woosley 1993). The associations of some GRBs with Type Ic supernovae (Woosely & Bloom 2006) favor a small-size progenitor star, likely a Wolf-Rayet (WR) star with striped hydrogen and helium envelopes. A successful jet is possible only when the accretion time scale is longer than the time scale for the jet to penetrate through the stellar envelope (MacFadyen & Woosley 1999; Waxman & Mészáros 2003; Bromberg et al. 2012). As a result, collapsar-related GRBs are typically “long”. On the other hand, a long duration does not necessarily refer to a large progenitor, since various mechanisms (e.g. fragmentation or magnetic barrier, King et al. 2005; Perna et al. 2006; Proga & Zhang 2006; Liu et al. 2012) can halt accretion temporarily and extend the total duration of accretion. Indeed, when X-ray flares are included, the central engine activity time of many GRBs can be much longer than the duration of gamma-ray emission itself (e.g. Burrows et al. 2005; Qin et al. 2013). GRB 121027A presents an extreme case of such a long-lasting central engine activity: Not only the X-ray flaring ac-

tivity extends to a much later time, but the total energetics of the flares is one order of magnitude higher than that of prompt emission. This demands that a significant amount of mass is accreted to the black hole in a later epoch. To reserve a large mass reservoir at later times, one would demand a large progenitor star than WRs. Since an un-mixed star would have an onion structure and would not store a large mass in the outer layer, this burst would also favor a progenitor star with a mixed envelope (Woosley & Heger 2006), as expected for a low-metallicity, rapidly-rotating star. Accretion of such a mixed envelope tends to be smooth (Kumar et al. 2008; Perna & MacFadyen 2010), but fragmentation or magnetic barrier (Perna et al. 2006; Proga & Zhang 2006; Liu et al. 2012) can modulate the accretion rate to power flares. Indeed a detailed fall-back model (Wu et al. 2013) can interpret the X-ray lightcurve of this burst well.

We search for similar GRBs from the *Swift* GRB archive. We find that the late XRT lightcurves of some GRBs are dominated by flares without the detection of power-law afterglow component up to $\sim 10^5$. These include GRBs 050502B, 050724, 050904, 050916, and 060223. The most prominent one is GRB 050904 (Cusumano et al. 2007). We compare the lightcurve of GRB 050904 with GRB 121027A in Fig. 4. One can observe that it is almost a carbon copy of GRB 121027A. These bursts may also have a large-size progenitor as GRB 121027A. A large progenitor was also suggested by Levan et al. (2013), who connect GRB 121027A with several other ultra-long GRBs, such as GRB 101225A and GRB 111209A. We note that many more GRBs have comparable or even longer duration of central engine activity (e.g. Qin et al. 2013). It is the energetics of the flares that matters the most in favor of a large progenitor.

The X-ray flux up to $T_0 + 3 \times 10^6$ seconds (~ 34 days post the GRB trigger) decays as $t^{-1.55}$ after the plateau. The spectral index of the X-rays is $\beta \sim 1.5$. This is roughly consistent with the expectation of the standard external shock model in the slow cooling regime for the wind medium case. No jet break is observed in the X-ray lightcurve. We place a lower limit of the half-opening angle (θ_j) of the jet. In the wind medium, one has $\theta_j > 0.202[t_{j,d}/(1+z)]^{1/4} \times (A\eta/E_{X,iso,52})^{1/4}$, where $t_{j,d} = t_j/1$ day, $\eta = 0.2$ (the radiative efficiency), $E_{X,iso,52} = E_{X,iso}/10^{52}$, and A is wind medium parameter for a profile $n = 5 \times 10^{11} Ar^{-2} \text{ g cm}^{-3}$ (e.g., Firmani et al. 2006). We take $A = 1$ that corresponds to a wind mass loss rate $\dot{M}_w = 10^{-5} M_\odot \text{ yr}^{-1}$ and a wind velocity $\dot{v}_w = 10^3 \text{ km s}^{-1}$. The derived θ_j is $> 10.4^\circ$, which is roughly consistent with that derived from the jet breaks observed in the optical bands (e.g., Bloom et al. 2003).

5. CONCLUSION

We have presented a temporal and spectral analysis of GRB 121027A observed with BAT and XRT. While the

prompt emission duration as detected by BAT is only 62.6 ± 4.8 s, extremely bright flares in the XRT band last up to $\sim 10^5$ s post the GRB trigger. Beyond, the external shock was observed up to more than 34 days without detection of a jet break.

A special property of GRB 121027A is that the total energy of late X-ray flares is one order of magni-

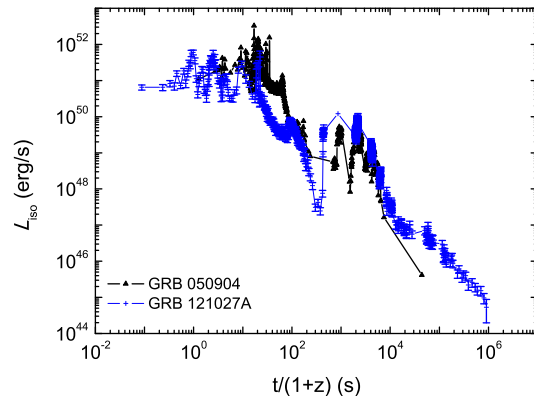


FIG. 4.— Comparison of the lightcurves of GRB 121027A with GRB 050904 in the 0.3–10 keV band in the rest frame.

tude higher than that of prompt emission. Yet, the radiation properties of X-ray flares seem to follow the same $L_{iso} - E_p$ and $\Gamma - L_{iso}$ empirical correlations with prompt gamma-ray emission, suggesting the same radiation mechanism (likely synchrotron) in the two phases. The large energy budget at a late epoch demands a large-size progenitor star, probably with mixed envelope layers. These progenitors may be different from the WR progenitor invoked to interpret most long GRBs. These GRBs form a distinct sub-category of long GRBs, another prototype of which is GRB 050904. These results suggest that the GRB progenitors can be diverse, not limited to a narrow channel. Future observations of possible associated SNe of these sub-category of GRBs would be of great value to infer the exact nature of their progenitor stars.

ACKNOWLEDGMENTS

We thank helpful discussion with Xue-Feng Wu and Zi-Gao Dai. This work made use of data supplied by the UK Swift Science Data Centre at the University of Leicester. This work is supported by the “973” Program of China (2009CB824800), the National Natural Science Foundation of China (Grants No. 11025313 and 11063001), Special Foundation for Distinguished Expert Program of Guangxi, the Guangxi Natural Science Foundation (2010GXNSFA013112, 2010GXNSFC013011, and Contract No. 2011-135). BZ acknowledges support from NSF (AST-0908362).

REFERENCES

- Amati, L., Frontera, F., Tavani, M., et al. 2002, A&A, 390, 81
- Beloborodov, A. M. 2010, MNRAS, 407, 1033
- Bloom, J. S., Frail, D. A., & Kulkarni, S. R. 2003, ApJ, 594, 674
- Bromberg, O., Nakar, E., Piran, T., & Sari, R. 2012, ApJ, 749, 110
- Burrows, D. N., Romano, P., Falcone, A., et al. 2005, Science, 309, 1833
- Butler, N. R., & Kocevski, D. 2007, ApJ, 663, 407
- Chincarini, G., Moretti, A., Romano, P., et al. 2007, ApJ, 671, 1903

TABLE 1

COMPARISON OF SPECTRAL FIT RESULTS WITH THE ABSORBED CUTOFF POWER LAW MODEL AND THE SINGLE POWER-LAW MODEL FOR GRB 121027A. THE RESULTS OF MODELS WITH “ \checkmark ” ARE ACCEPTED FOR OUR ANALYSIS.

Interval(s)	model	Γ_c	$E_c(\text{keV})$	C-Stat/dof	model	Γ	C-Stat/dof
1-74	cpl(\checkmark)	$1.49^{+0.11}_{-0.12}$	$93.30^{+55.82}_{-27.14}$	88.7/490	pl	$1.74^{+0.05}_{-0.06}$	111.2/491
77-97	cpl(\checkmark)	$0.66^{+0.27}_{-0.28}$	$2.03^{+0.67}_{-0.44}$	350.3/489	pl	1.71 ± 0.08	404.0/490
97-121	cpl(\checkmark)	$1.12^{+0.31}_{-0.33}$	$2.38^{+1.36}_{-0.68}$	305.3/435	pl	1.94 ± 0.09	329.1/436
150-260	cpl(\checkmark)	$1.41^{+0.20}_{-0.21}$	$2.16^{+0.72}_{-0.46}$	403.9/577	pl	$2.22^{+0.10}_{-0.06}$	460.4/578
260-505	cpl	$2.14^{+0.14}_{-0.15}$	$5.95^{+5.23}_{-1.96}$	404.5/648	pl(\checkmark)	2.43 ± 0.05	417.5/649
1172-1216	cpl	$1.19^{+0.31}_{-0.33}$	$6.68^{+47.11}_{-3.26}$	290.4/508	pl(\checkmark)	1.53 ± 0.10	293.9/509
5404-6082	cpl(\checkmark)	1.21 ± 0.05	$7.33^{+1.33}_{-0.99}$	783.3/821	pl	1.52 ± 0.02	904.2/822
11112-11883	cpl(\checkmark)	1.68 ± 0.10	$7.68^{+4.07}_{-2.02}$	626.5/630	pl	1.95 ± 0.03	650.1/631
16347-17659	cpl	$1.90^{+0.31}_{-0.32}$	$5.92^{+50.16}_{-2.91}$	248.5/489	pl(\checkmark)	2.22 ± 0.10	251.8/490
22798-23598	pl(\checkmark)	2.91 ± 0.20	125.6/461
28396-30083	pl(\checkmark)	$2.69^{+0.16}_{-0.15}$	190.1/427
35290-76224	pl(\checkmark)	2.48 ± 0.15	188.0/425
138272-201989	pl(\checkmark)	2.17 ± 0.15	196.3/242
328262-485712	pl(\checkmark)	$2.52^{+0.21}_{-0.20}$	120.8/417
664241-2298128	pl(\checkmark)	$2.57^{+0.29}_{-0.27}$	113.5/319

- Colgate, S. A. 1974, ApJ, 187, 333
 Cusumano, G., Mangano, V., Chincarini, G., et al. 2007, A&A, 462, 73
 Dai, Z. G., Wang, X. Y., Wu, X. F., & Zhang, B. 2006, Science, 311, 1127
 Evans, P. A., Beardmore, A. P., Page, K. L., et al. 2009, MNRAS, 397, 1177
 Evans, P. A., Gronwall, C., Krimm, H. A., et al. 2012, GRB Coordinates Network, 13906, 1
 Falcone, A. D., Morris, D., Racusin, J., et al. 2007, ApJ, 671, 1921
 Fan, Y. Z., & Wei, D. M. 2005, MNRAS, 364, L42
 Fan, Y. Z., Zhang, B., & Proga, D. 2005, ApJ, 635, L129
 Firmani, C., Ghisellini, G., Avila-Reese, V., & Ghirlanda, G. 2006, MNRAS, 370, 185
 King, A., O’Brien, P. T., Goad, M. R., et al. 2005, ApJ, 630, L113
 Kumar, P., Narayan, R., & Johnson, J. L. 2008, Science, 321, 376
 Lü, J., Zou, Y.-C., Lei, W.-H., et al. 2012, ApJ, 751, 49
 Lazzati, D., & Perna, R. 2007, MNRAS, 375, L46
 Lei, W.-H., Zhang, B., & Liang, E.-W. 2012, arXiv:1209.4427
 Levan, A. J., Tanvir, N. R., Starling, R. L. C., et al. 2013, arXiv:1302.2352
 Liang, E. W., Dai, Z. G., & Wu, X. F. 2004, ApJ, 606, L29
 Liang, E.-W., Lü, H.-J., Hou, S.-J., Zhang, B.-B., & Zhang, B. 2009, ApJ, 707, 328
 Liang, E.-W., Yi, S.-X., Zhang, J., et al. 2010, ApJ, 725, 2209
 Liang, E.-W., Zhang, B.-B., & Zhang, B. 2007, ApJ, 670, 565
 Liu, T., Liang, E.-W., Gu, W.-M., et al. 2012, ApJ, 760, 63
 Lloyd, N. M., & Petrosian, V. 2000, ApJ, 543, 722
 Lu, R.-J., Wei, J.-J., Liang, E.-W., et al. 2012, ApJ, 756, 112
 MacFadyen, A. I., & Woosley, S. E. 1999, ApJ, 524, 262
 Meszaros, P., Rees, M. J., & Papathanassiou, H. 1994, ApJ, 432, 181
 Nousek, J. A., Kouveliotou, C., Grupe, D., et al. 2006, ApJ, 642, 389
 Peng, F. K., et al. 2013, J. Astro., Astrophys., accepted
 Perna, R., Armitage, P. J., & Zhang, B. 2006, ApJ, 636, L29
 Perna, R., & MacFadyen, A. 2010, ApJ, 710, L103
 Proga, D., & Zhang, B. 2006, MNRAS, 370, L61
 Qin, Y., Liang, E.-W., Liang, Y.-F., et al. 2013, ApJ, 763, 15
 Rees, M. J., & Mészáros, P. 2005, ApJ, 628, 847
 Serino, M., Nakahira, S., Negoro, H., et al. 2012, GRB Coordinates Network, 13908, 1
 Thompson, C. 1994, MNRAS, 270, 480
 Waxman, E., & Mészáros, P. 2003, ApJ, 584, 390
 Woosley, S. E. 1993, ApJ, 405, 273
 Woosley, S. E., & Bloom, J. S. 2006, ARA&A, 44, 507
 Woosley, S. E., & Heger, A. 2006, ApJ, 637, 914
 Wu, X. F., et al. 2013, ApJ, submitted
 Yonetoku, D., Murakami, T., Nakamura, T., et al. 2004, ApJ, 609, 935
 Zhang, B.-B., Liang, E.-W., & Zhang, B. 2007, ApJ, 666, 1002
 Zhang, B., Fan, Y. Z., Dyks, J., et al. 2006, ApJ, 642, 354
 Zhang, B., & Yan, H. 2011, ApJ, 726, 90
 Zou, Y. C., Dai, Z. G., & Xu, D. 2006, ApJ, 646, 1098